Mecánica Computacional Vol. XXI, pp. 1504–1516
S. R. Idelsohn, V. E. Sonzogni and A. Cardona (Eds.)
Santa Fe–Paraná, Argentina, October 2002

ON A MIXED FINITE ELEMENT FORMULATION FOR PLANE ELASTICITY

Claudio E. Jouglard

Laboratorio de Mecánica Computacional. Departamento de Física.
Facultad de Ingeniería. Universidad de Buenos Aires.
Av. Paseo Colón 850, (1063) Buenos Aires, Argentina
e-mail: cjougla@fi.uba.ar.

Key words: Mixed Finite Elements, Elasticity, Computational Methods.

Abstract. *In this work we present some numerical results for a mixed finite element formulation for elasticity problems. In particular we have tested a triangular finite element with linear interpolation for both displacements and strains. We use the displacements at vertices and a combination of stresses and strains at mid-side points as nodal variables. A static condensation technique was employed that rendered a finite element formulation with only nodal displacements as degrees of freedom. Some comparisons are made with other conventional elements that show the high performance of the mixed element.*

1 INTRODUCTION

For 2D finite element models the quadrilateral element is preferred, since it has a better performance when compared with triangular elements[1]. But unstructured mesh generation of quadrilateral meshes is more difficult than that of triangles. So, an efficient triangle is desirable since it could be incorporated easily in adaptive mesh generation codes.

For elasticity problems the conventional formulation of triangles based on displacements has several limitations when compared with quadrilateral elements based on the same formulation, especially for low order elements. A mixed formulation where displacements and strains are interpolated independently can overcome these limitations.

In this work we analyze a mixed formulation for triangles based on a linear interpolation of displacements and strains. Originally[2,3] this element used as nodal connectors the vertex displacements and the midside stresses. We will show that with an adequate choice of the connectors some orthogonality properties arise in the formulation that give an element with only vertex displacement as degrees of freedom. As it will be shown in the numerical examples the performance of this element is very satisfactory when compared with conventional triangles and quadrilaterals with the same degrees of freedom.

2 MIXED FINITE ELEMENT FORMULATION FOR ELASTICITY

2.1 Hellinger-Reissner Principle

We start with the Hellinger-Reissner principle

$$\Pi_{HR} = \int_\Omega \boldsymbol{\varepsilon}^T \mathbf{D}\,\mathbf{S}\,\mathbf{u}\,d\Omega - \tfrac{1}{2}\int_\Omega \boldsymbol{\varepsilon}^T \mathbf{D}\,\boldsymbol{\varepsilon}\,d\Omega - \int_\Omega \mathbf{u}^T \mathbf{b}\,d\Omega - \int_{\Gamma_\sigma} \mathbf{u}^T \mathbf{t}\,d\Gamma \tag{1}$$

where Ω is a bidimensional domain with a displacement field $\mathbf{u} = \{u, v\}$ and domain loads $\mathbf{b} = (b_x, b_y)$ and boundary tractions $\mathbf{t} = (t_x, t_y)$ on the portion Γ_σ of the boundary. The strain vector $\boldsymbol{\varepsilon}$ is defined as

$$\boldsymbol{\varepsilon} = \{\varepsilon_x \;\; \varepsilon_y \;\; \gamma_{xy}\}^T \tag{2}$$

and are related with the displacements $\mathbf{u}$ by the first order strain differential operator $\boldsymbol{S}$ as

$$\boldsymbol{\varepsilon} = \boldsymbol{S}\,\mathbf{u} \tag{3}$$

where $\boldsymbol{S}$ is defined as

$$\mathbf{S} = \begin{bmatrix} \dfrac{\partial}{\partial x} & 0 & \dfrac{\partial}{\partial y} \\ 0 & \dfrac{\partial}{\partial y} & \dfrac{\partial}{\partial x} \end{bmatrix}^T \tag{4}$$

The stress vector $\boldsymbol{\sigma}$ is defined as

$$\boldsymbol{\sigma} = \{\sigma_x \;\; \sigma_y \;\; \tau_{xy}\}^T \tag{5}$$

The stress vector $\boldsymbol{\sigma}$ is related with the strain vector $\boldsymbol{\varepsilon}$ by the matrix $\mathbf{D}$ of elastic constants as

$$\boldsymbol{\sigma} = \mathbf{D}\,\boldsymbol{\varepsilon} = \mathbf{D}\boldsymbol{S}\,\mathbf{u} \tag{6}$$

For plane strain problems the matrix $\mathbf{D}$ is given as

$$\mathbf{D} = \frac{E}{(1+\nu)(1-2\nu)}\begin{bmatrix} 1-\nu & \nu & 0 \\ \nu & 1-\nu & 0 \\ 0 & 0 & \dfrac{(1-2\nu)}{2} \end{bmatrix} \tag{7}$$

where E is the elastic modulus and ν is Poisson's ratio.

The stationarity of the Hellinger-Reissner functional for arbitrary variations $\delta\boldsymbol{\varepsilon}$ and $\delta\mathbf{u}$ gives

$$\begin{aligned}\delta\Pi_{HR} = &\int_\Omega \delta\boldsymbol{\varepsilon}^T \mathbf{D}\,\mathbf{S}\,\mathbf{u}\,d\Omega + \int_\Omega \boldsymbol{\varepsilon}^T \mathbf{D}\,\mathbf{S}\,\delta\mathbf{u}\,d\Omega - \int_\Omega \delta\boldsymbol{\varepsilon}^T \mathbf{D}\,\boldsymbol{\varepsilon}\,d\Omega \\ &- \int_\Omega \delta\mathbf{u}^T \mathbf{b}\,d\Omega - \int_{\Gamma_\sigma} \delta\mathbf{u}^T \mathbf{t}\,d\Gamma = 0\end{aligned} \tag{8}$$

Introducing the finite element approximations

$$\begin{aligned}\boldsymbol{\varepsilon} &= \boldsymbol{N}_{\boldsymbol{\varepsilon}}\,\boldsymbol{\varepsilon}_{\mathbf{e}} \\ \mathbf{u} &= \boldsymbol{N}_{\boldsymbol{u}}\,\mathbf{u}_{\mathbf{e}}\end{aligned} \tag{9}$$

where $\mathbf{u_e}$ are the displacements at vertices and $\boldsymbol{\varepsilon_e}$ are the strains at midside points. $\boldsymbol{N_u}$ are the standard linear shape functions, and $\boldsymbol{N_\varepsilon}$ are linear shape functions continuous at midside points (see figure 1). It can be shown that these shape functions are orthogonal [4].

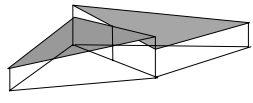

Figure 1: Linear shape functions for strain interpolation.

After replacing the variations

$$\begin{aligned}\delta\boldsymbol{\varepsilon} &= \boldsymbol{N}_{\boldsymbol{\varepsilon}}\,\delta\boldsymbol{\varepsilon}_{\mathbf{e}} \\ \delta\mathbf{u} &= \boldsymbol{N}_{\boldsymbol{u}}\,\delta\mathbf{u}_{\mathbf{e}}\end{aligned} \tag{10}$$

in the Hellinger-Reissner functional we have

$$\begin{aligned}\delta\Pi_{HR} = &\sum_e \left(\int_{\Omega_e} \delta\boldsymbol{\varepsilon}_e^T \mathbf{N}_\varepsilon^T \mathbf{D}\,\mathbf{S}\,\mathbf{N}_u \mathbf{u}_e\,d\Omega - \int_{\Omega_e} \delta\boldsymbol{\varepsilon}_\varepsilon^T \mathbf{N}_\varepsilon^T \mathbf{D}\,\mathbf{N}_\varepsilon\,\boldsymbol{\varepsilon}_e\,d\Omega \right) \\ &+ \sum_e \left(\int_{\Omega_e} \delta\mathbf{u}_e^T \mathbf{N}_u^T \mathbf{S}^T \mathbf{D}\,\mathbf{N}_\varepsilon\,\boldsymbol{\varepsilon}_e\,d\Omega - \int_{\Omega_e} \delta\mathbf{u}_e^T \mathbf{N}_u^T \mathbf{b}\,d\Omega - \int_{\Gamma_{\sigma e}} \delta\mathbf{u}_e^T \mathbf{N}_u^T \mathbf{t}\,d\Gamma \right) = 0\end{aligned} \tag{11}$$

where we have replaced the integrals by sums of integrals over all the elements of the mesh.

2.2 Choice of element connectors

For each element we define positive directions for the normal and tangential axes of each side. In particular we adopt as positive the outward normal and the clockwise tangential directions as shown in figure 2.

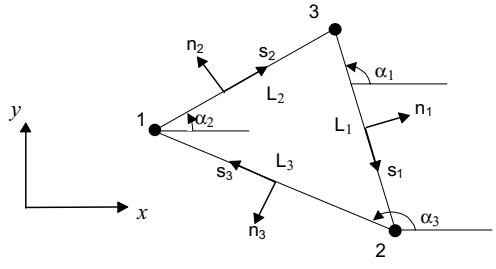

Figure 2: Tangential and normal axes of each side.

Then we can define a local stress vector $\boldsymbol{\sigma}_L$ on each side

$$\boldsymbol{\sigma}_L = \{\sigma_s \;\; \sigma_n \;\; \tau_{ns}\}^T \tag{12}$$

where σ_s, σ_n, τ_{ns} are the components of the stress vector for the local axes of each side (see figure 3).

Also, we can define a local strain vector $\boldsymbol{\varepsilon}_L$ on each side

$$\boldsymbol{\varepsilon}_L = \{\varepsilon_s \;\; \varepsilon_n \;\; \gamma_{ns}\}^T \tag{13}$$

These strains and stresses are related by the matrix **D** as

$$\boldsymbol{\sigma}_L = \mathbf{D}\,\boldsymbol{\varepsilon}_L \tag{14}$$

If we analyze the stresses acting on the interface between elements, and assuming the same thickness for adjacent elements, by equilibrium we must have continuity of the components σ_n and τ_{ns} between elements.

Remark 1: If the thickness if different between adjacent elements we must have continuity of the normal and tangential forces by unit of length along the sides, that is

$$F_n = \sigma_n h \quad , \quad F_s = \tau_{ns} h \tag{15}$$

where h is the element thickness and F_n , F_s are the normal and tangential forces by unit of length along the sides, respectively. For simplicity we will assume constant thickness in the domain.

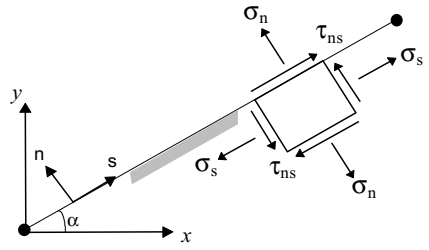

Figure 3: Tangential and normal stresses for local axes of each side.

Also, the tangential displacement u_s along each side is a continuous function, this implies that the component ε_s of the strain vector is a continuous function too, since it is defined as

$$\varepsilon_s = \frac{\partial u_s}{\partial s} \tag{16}$$

We must note that if adjacent elements are composed of different materials, imposing the continuity of all the components of the strain vector between elements at midside points is not a valid assumption, instead we must impose the continuity of a combination of local strains and stresses given by

$$\boldsymbol{\phi}_L = \{\varepsilon_s \;\; \sigma_n \;\; \tau_{ns}\}^T \tag{17}$$

This vector is related with the local strain vector $\boldsymbol{\varepsilon}_L$ as

$$\boldsymbol{\varepsilon}_L = \mathbf{T}_\varepsilon \, \boldsymbol{\phi}_L \tag{18}$$

where for plane strain the matrix $\mathbf{T}_\varepsilon$ is

$$\mathbf{T}_\varepsilon = \begin{bmatrix} 1 & 0 & 0 \\ -\dfrac{\nu}{(1-\nu)} & \dfrac{(1+\nu)(1-2\nu)}{(1-\nu)E} & 0 \\ 0 & 0 & \dfrac{2(1+\nu)}{E} \end{bmatrix} \tag{19}$$

The local strain vector $\boldsymbol{\varepsilon}_L$ on each side L is related with the global strain vector $\boldsymbol{\varepsilon}$ as

$$\boldsymbol{\varepsilon} = \mathbf{T}_{\alpha L} \, \boldsymbol{\varepsilon}_L \tag{20}$$

where the rotation matrix $\mathbf{T}_{\alpha L}$ for side L is

$$\mathbf{T}_{\alpha L} = \begin{bmatrix} \cos^2\alpha_L & \sin^2\alpha_L & -\sin\alpha_L\,\cos\alpha_L \\ \sin^2\alpha_L & \cos^2\alpha_L & \sin\alpha_L\,\cos\alpha_L \\ 2\sin\alpha_L\,\cos\alpha_L & -2\sin\alpha_L\,\cos\alpha_L & \cos^2\alpha_L - \sin^2\alpha_L \end{bmatrix} \tag{21}$$

Then the vector $\boldsymbol{\varepsilon}$ of global strains at midside points of side L can be expressed in terms of the vector of unknowns $\boldsymbol{\phi}_L$ as

$$\boldsymbol{\varepsilon} = \mathbf{T}_{\alpha L}\,\mathbf{T}_{\varepsilon}\,\boldsymbol{\phi}_L \tag{22}$$

and its variations for each side are

$$\delta\boldsymbol{\varepsilon} = \mathbf{T}_{\alpha L}\,\mathbf{T}_{\varepsilon}\,\delta\boldsymbol{\phi}_L \tag{23}$$

2.3 Matrices of the mixed formulation

If we substitute equations (22), (23) in (11) we obtain for arbitrary variations $\delta\boldsymbol{\phi}_L$, $\delta\mathbf{u}$ the next system of equations typical of mixed formulations

$$\left[\begin{array}{c:c} -\mathbf{A} & \mathbf{C} \\ \hdashline \mathbf{C}^T & \mathbf{0} \end{array}\right] \left\{\begin{array}{c} \boldsymbol{\phi} \\ \hdashline \mathbf{u} \end{array}\right\} = \left\{\begin{array}{c} \mathbf{0} \\ \hdashline \mathbf{f} \end{array}\right\} \tag{24}$$

where each matrix is composed by the sum over all the elements, that is

$$\mathbf{A} = \sum_e \mathbf{A}^e \qquad \mathbf{C} = \sum_e \mathbf{C}^e \qquad \mathbf{f} = \sum_e \mathbf{f}^e \tag{25}$$

and

$$\mathbf{A}^e = \begin{bmatrix} \mathbf{A}^e_{11} & \mathbf{A}^e_{12} & \mathbf{A}^e_{13} \\ & \mathbf{A}^e_{22} & \mathbf{A}^e_{23} \\ \textit{Symmetric} & & \mathbf{A}^e_{33} \end{bmatrix} \quad \mathbf{C}^e = \begin{bmatrix} \mathbf{C}^e_{11} & \mathbf{C}^e_{12} & \mathbf{C}^e_{13} \\ \mathbf{C}^e_{11} & \mathbf{C}^e_{22} & \mathbf{C}^e_{23} \\ \mathbf{C}^e_{31} & \mathbf{C}^e_{32} & \mathbf{C}^e_{33} \end{bmatrix} \quad \mathbf{f}^e = \begin{Bmatrix} \mathbf{f}^e_1 \\ \mathbf{f}^e_2 \\ \mathbf{f}^e_3 \end{Bmatrix} \tag{26}$$

with

$$\begin{aligned} \mathbf{A}^e_{ij} &= \int_{\Omega_e} \boldsymbol{T}^T_{\varepsilon}\,\boldsymbol{T}^T_{\alpha i}\,\mathbf{N}^T_{\varepsilon i}\,\mathbf{D}\,\mathbf{N}_{\varepsilon j}\,\boldsymbol{T}_{\alpha j}\,\boldsymbol{T}_{\varepsilon}\,\mathrm{d}\Omega \\ \mathbf{C}^e_{ij} &= \int_{\Omega_e} \boldsymbol{T}^T_{\varepsilon}\,\boldsymbol{T}^T_{\alpha i}\,\mathbf{N}^T_{\varepsilon i}\,\mathbf{D}\,\mathbf{S}\,\mathbf{N}_{uj}\,\mathrm{d}\Omega \\ \mathbf{f}^e_i &= \int_{\Omega_e} \mathbf{N}^T_{ui}\,\mathbf{b}\,\mathrm{d}\Omega + \int_{\Gamma_{\sigma e}} \mathbf{N}^T_{ui}\,\mathbf{t}\,\mathrm{d}\Gamma \end{aligned} \tag{27}$$

where $\mathbf{N}_{uj}$ is the matrix of shape functions for the displacements at vertex j, that is

$$\mathbf{N}_{uj} = \begin{bmatrix} N_j & 0 \\ 0 & N_j \end{bmatrix} \tag{28}$$

and $\mathbf{N}_{\varepsilon i}$ is the matrix of shape functions for the strains at side *i*, that is

$$\mathbf{N}_{\varepsilon i} = \begin{bmatrix} M_i & 0 & 0 \\ 0 & M_i & 0 \\ 0 & 0 & M_i \end{bmatrix} \tag{29}$$

These shape functions can be expressed using area coordinates [4] as

$$\begin{aligned} M_i &= 1 - 2\xi_i \\ N_j &= \xi_j \end{aligned} \tag{30}$$

If we assume constant material properties for each element, we have

$$\begin{aligned} \mathbf{A}_{ij}^e &= \left(\int_{\Omega_e} M_i \, M_j \, \mathrm{d}\Omega \right) \boldsymbol{T}_\varepsilon^T \boldsymbol{T}_{\alpha i}^T \mathbf{D} \, \boldsymbol{T}_{\alpha j} \, \boldsymbol{T}_\varepsilon \\ \mathbf{C}_{ij}^e &= \left(\int_{\Omega_e} M_i \, \mathrm{d}\Omega \right) \boldsymbol{T}_\varepsilon^T \boldsymbol{T}_{\alpha i}^T \mathbf{D} \, \mathbf{S} \, \mathbf{N}_{uj} \end{aligned} \tag{31}$$

The complete expressions of these matrices can be found in appendix A.

Due to the orthogonality properties of the shape functions M_i the matrices $\mathbf{A}_{ij}$ with $i \neq j$ are null. Also, the choice of the connectors gives *diagonal* matrices $\mathbf{A}_{ii}$, this implies that the complete matrix **A** is a *diagonal* matrix too and can be easily inverted. It should be noted that matrix **A** is also positive definite for values of $\nu<0.5$.

Remark 2: If the material of the element is anisotropic, the matrices $\mathbf{A}_{ij}$ with $i \neq j$ are still null but now matrices $\mathbf{A}_{ii}$ are full matrices of size 3 x 3. Then in this case the matrix **A** is a block diagonal matrix that can be easily inverted too.

2.4 Assembling of the stiffness matrix

If we explicit ϕ for the first of (24) we have

$$\phi = \mathbf{A}^{-1}\mathbf{C}\mathbf{u} \tag{32}$$

and replacing this vector in the second of (24) we obtain

$$\left(\mathbf{C}^T \mathbf{A}^{-1} \mathbf{C}\right)\mathbf{u} = \mathbf{K}\mathbf{u} = \mathbf{f} \tag{33}$$

where

$$\mathbf{K} = \mathbf{C}^T \mathbf{A}^{-1} \mathbf{C} \tag{34}$$

is the stiffness matrix.

Since matrix **A** is diagonal, its inverse $\mathbf{A}^{-1}$ is also a diagonal matrix whose elements are the inverse of the elements of **A**.

The matrix **K** is composed of submatrices $\mathbf{K}_{ij}$ of size 2x2 relating the displacements of vertices *i* and *j*. This submatrices can be expressed as

$$\mathbf{K}_{ij} = \sum_{l} \mathbf{C}_{li}^{T}\, \mathbf{A}_{ll}^{-1}\, \mathbf{C}_{lj} \tag{35}$$

Note that matrices $\mathbf{C}_{li}$ are different from zero only if side l and vertex i belong the same element. Then the stiffness matrix $\mathbf{K}$ can be easily assembled by looping over all the sides and a data structure based on sides is preferable.

We must eliminate from the system (24) those equations associated with boundary conditions. We can have specified values for the variables $\boldsymbol{\phi}_R$ of the vector $\boldsymbol{\phi}$ and for the displacements $\mathbf{u}_R$ of the vector $\mathbf{u}$, then the system (24) can be written as

$$\begin{bmatrix} -\mathbf{A}_R & \mathbf{0} & \mathbf{C}_{RR} & \mathbf{C}_{RF} \\ \mathbf{0} & -\mathbf{A}_F & \mathbf{C}_{FR} & \mathbf{C}_{FF} \\ \mathbf{C}_{RR}^{T} & \mathbf{C}_{FR}^{T} & \mathbf{0} & \mathbf{0} \\ \mathbf{C}_{RF}^{T} & \mathbf{C}_{FF}^{T} & \mathbf{0} & \mathbf{0} \end{bmatrix} \begin{Bmatrix} \boldsymbol{\phi}_R \\ \boldsymbol{\phi}_F \\ \mathbf{u}_R \\ \mathbf{u}_F \end{Bmatrix} = \begin{Bmatrix} \mathbf{0} \\ \mathbf{0} \\ \mathbf{f}_R \\ \mathbf{f}_F \end{Bmatrix} \tag{36}$$

where $\boldsymbol{\phi}_F$ and $\mathbf{u}_F$ are the free degrees of freedom of the system.

From the second equation we have

$$\boldsymbol{\phi}_F = \mathbf{A}_F^{-1}\left[\mathbf{C}_{FF}\mathbf{u}_F + \mathbf{C}_{FR}\mathbf{u}_R\right] \tag{37}$$

and replacing this equation in the last equation of (36) we have

$$\mathbf{C}_{FF}^{T}\, \mathbf{A}_F^{-1}\, \mathbf{C}_{FF}\, \mathbf{u}_F = \mathbf{f}_F - \mathbf{C}_{RF}^{T}\boldsymbol{\phi}_R - \mathbf{C}_{FF}^{T}\, \mathbf{A}_F^{-1}\, \mathbf{C}_{FR}\, \mathbf{u}_R \tag{38}$$

Then we must modify the load vector to take into consideration the contribution of the restricted degrees of freedom.

2.5 Recovering of stress and strain

From equation (38) we can obtain the displacements $\mathbf{u}_F$ independently of the unknown stresses and strains in $\boldsymbol{\phi}_F$, then to obtain these unknowns we must use equation (37).

An in depth inspection of this equation reveals the next relations that must be satisfied by the unknowns ε_{si}, σ_{ni}, τ_{nsi} on each side L_i

$$\begin{aligned} \varepsilon_{si} &= \frac{u_{s2} - u_{s1}}{L_i} \\ \sigma_{ni} &= \frac{A_1\, \sigma_{n1}^{*} + A_2\, \sigma_{n2}^{*}}{A_1 + A_2} \\ \tau_{nsi} &= \frac{A_1\, \tau_{ns1}^{*} + A_2\, \tau_{ns2}^{*}}{A_1 + A_2} \end{aligned} \tag{39}$$

where u_{s1}, u_{s2} are the displacements and the ends of side L_i. A_1, A_2 are the areas of the elements adjacent to the side and σ_n^{*}, τ_{ns}^{*} are the stresses on each of these elements obtained from the

derivatives of a linear displacement field interpolated from the vertex values of displacements.

The first of these equations indicates that the axial strain ε_{si} at a midside point can be obtained from the derivatives of a linear displacement field along the side. As it well known from the mean value theorem this recovered value is superconvergent at that point.

The second and third equations indicates that the stresses σ_{ni}, τ_{nsi} at a midside point can be obtained as a weighted average sum of the constant stresses on each element adjacent to the side using the area of each element as weighting factor.

Remark 3: These midside values can be used to define a smoothed stress field for linear triangles based on a displacement formulation. In reference 5 an error estimator for linear triangles has been constructed from smoothed stresses obtained at midsides points, but using only simple averaging. This estimator showed an excellent performance when compared with other well known error estimators.

As noted in figure 1 the recovered strain and stress fields are only continuos at midside points, a completely continuous stress field can be constructed by nodal averaging of the computed stresses, but the amount of discontinuity of the recovered stresses can be useful as an error measure [3].

3 NUMERICAL RESULTS

For comparison purposes we have used a plane strain elasticity problem [4] on the domain described in figure 4.

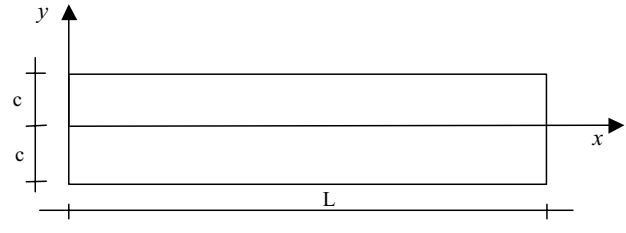

Figure 4: Domain for plane strain elasticity problem.

The boundary conditions for displacements are

$$u(0,0) = 0 \qquad v(0,0) = 0 \qquad u(0,\pm c) = 0 \tag{40}$$

and the boundary conditions for tractions are

$$\left.\begin{array}{l} t_x(x,\pm c)=0 \\ t_y(x,\pm c)=0 \end{array}\right\} x \text{ in } (0,L) \qquad \left.\begin{array}{l} t_x(L,y)=0 \\ t_y(L,y)=\dfrac{P}{2I}(c^2-y^2) \end{array}\right\} y \text{ in } (-c,c) \tag{41}$$

$$\left.\begin{array}{l} t_x(0,y)=\dfrac{PLy}{2I} \\ t_y(0,y)=-\dfrac{P}{2I}(c^2-y^2) \end{array}\right\} y \text{ in } (-c,c)$$

where P is a given constant and $I = 2c^3/3$.

The traction boundary conditions are those encountered in simple bending theory for a cantilever beam with a parabolically varying end shear.

We employ the following data in the calculations

$$P=1 \qquad L=16 \qquad c=2 \qquad E=1 \qquad \nu=0.3 \tag{42}$$

A series of three meshes with 6, 15 and 45 nodes has been used (fig. 5). Only half of the domain has been modeled since the x axis is a line of antisymmetry.

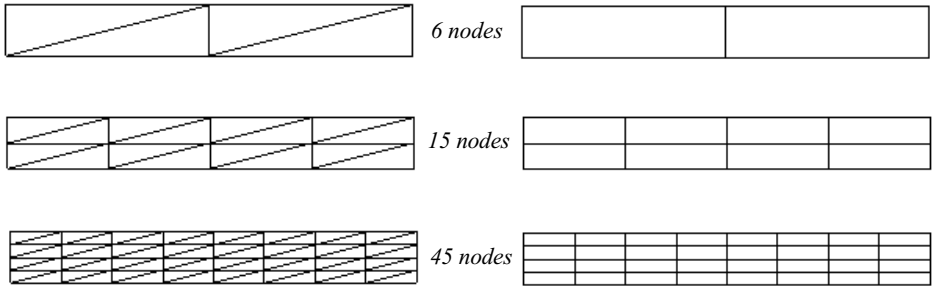

Figure 5: Meshes for the plane strain elasticity problem.

We have compared the vertical tip displacement, i.e. $v(L,0)$, for the mixed triangle (T3M), the linear triangle (T3) based on the displacement formulation and the bilinear quadrilateral (Q4) with 2 x 2 uniform integration. The results are shown in table 1 and figure 6.

Table 1: Normalized vertical tip displacement for plane strain problem.

nodes	T3	Q4	T3M
6	0.209	0.446	0.774
15	0.488	0.768	0.971
45	0.791	0.938	1.009

We can observe the excellent performance of the linear mixed triangle since in this case it

has the same precision of the bilinear quadrilateral but with only one third of the nodes.

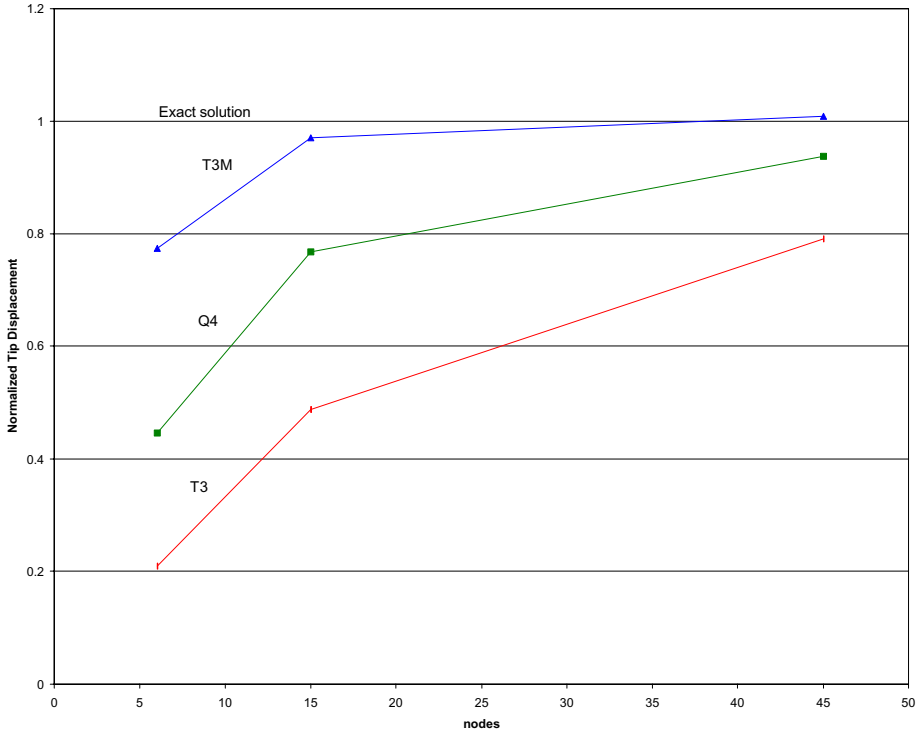

Figure 6: Normalized vertical tip displacement for plane strain problem.

Also we made a comparison for ν = 0.499 (*nearly incompressible case*) using the mesh of 45 nodes and the results are shown in table 2.

Table 2: Normalized vertical tip displacement for plane strain problem.

ν	T3	Q4	T3M
0.3	0.791	0.938	1.009
0.499	0.600	0.334	0.977

We note that the linear mixed triangle is also very robust in nearly incompressible situations and there is no need of applying special remedies[1,3,4], such as those employed for bilinear quadrilaterals to make this element of practical usefulness in nearly incompressible cases.

4 CONCLUSIONS

The results show that the presented linear mixed triangle has a very good performance when compared with bilinear quadrilaterals. It gives very good approximations with coarse meshes and is robust in incompressible cases. The appropriate choice of connectors simplifies the mixed formulation giving an element with only nodal displacements as degrees of freedom. It has been shown that unknown stresses on each side can be interpreted as a weighted average sum of the constant stresses on each element adjacent to that side. This element can be implemented efficiently in adaptive refinement codes coupled with unstructured mesh generators.

5 APPENDIX A

For each element of area A we have

$$\mathbf{A}_{ii}^{e} = \frac{(2A)}{6}\begin{bmatrix} \dfrac{E}{1-\nu^2} & 0 & 0 \\ 0 & \dfrac{(1+\nu)(1-2\nu)}{(1-\nu)E} & 0 \\ 0 & 0 & \dfrac{2(1+\nu)}{E} \end{bmatrix} \tag{A.1}$$

and using the notation defined in figure 2 we have

$$\mathbf{C}_{ij}^{e} = \frac{L_j}{6}\begin{bmatrix} C11_{ij} & C12_{ij} \\ C21_{ij} & C22_{ij} \\ C31_{ij} & C32_{ij} \end{bmatrix} \tag{A.2}$$

where

$$\begin{aligned} C11_{ij} &= \frac{E}{(1-\nu^2)} c_i\left(c_i s_j - s_i c_j\right) \\ C12_{ij} &= \frac{E}{(1-\nu^2)} s_i\left(c_i s_j - s_i c_j\right) \\ C21_{ij} &= \frac{1}{1-\nu}\left\{s_i\left(s_i s_j + c_i c_j\right) - \nu\left[s_j\left(s_i^2 - c_i^2\right) + c_j\left(2 s_i c_i\right)\right]\right\} \\ C22_{ij} &= \frac{1}{1-\nu}\left\{-c_i\left(s_i s_j + c_i c_j\right) + \nu\left[c_j\left(c_i^2 - s_i^2\right) + s_j\left(2 s_i c_i\right)\right]\right\} \\ C31_{ij} &= c_j\left(s_i^2 - c_i^2\right) - s_j\left(2 s_i c_i\right) \\ C32_{ij} &= s_j\left(c_i^2 - s_i^2\right) - c_j\left(2 s_i c_i\right) \end{aligned} \tag{A.3}$$

with

$$s_i = \frac{y_{jk}}{L_i} \qquad c_i = \frac{x_{jk}}{L_i} \tag{A.4}$$

$$x_{jk} = x_j - x_k \qquad y_{jk} = y_j - y_k$$

The other matrices are obtained by cyclic permutation of indices.

6 REFERENCES

[1] R.D. Cook, D.S. Malkus and M.E. Plesha, *Concepts and applications of finite element analysis*, John Wiley & Sons, 3rd edition, (1989).

[2] O.C. Zienkiewickz and D. Lefebvre, "Mixed methods for FEM and the patch test. Some recent developments", in *Analyse Mathematique of Application* (eds. F. Murat and O. Pironneau), Gauthier Villars, Paris (1988).

[3] O.C. Zienkiewicz and R.L. Taylor, *The finite element method*, McGraw Hill, Vol. I., 1989.

[4] T.J.R. Hughes, *The finite element method, linear static and dynamic finite element analysis*, Prentice-Hall International, 1987.

[5] C.E. Jouglard, "Un estimador de error simple para triángulos lineales", XII Congreso sobre Métodos Numéricos y sus aplicaciones, ENIEF 2001, (ed. F. Flores), 438-445 (2001).